Research Article

Serum Protein and ALT Profiles in Hormone-Induced Follicular Cyst Rat Models

Yudit Oktanella[1*], Nabilla Rizky Mahalita[2], Hana Ismiawati[3], Ragil Angga Prastiya[4]

[1]Department of Veterinary Reproduction, Faculty of Veterinary Medicine, Universitas Brawijaya, Malang, Indonesia; [2]Veterinary Clinic Tulungagung Petcare, Tulungagung, East Java, Indonesia; Veterinary Clinic KHJ Solo, Surakarta, Central Java, Indonesia; [3]Klinik Hewan KHJ Solo, Surakarta, Central Java, Indonesia; [4]Veterinary Professional Program, Department of Health and Life Sciences, Faculty of Health, Medicine, and Life Sciences (FIKKIA), Universitas Airlangga, Surabaya, Indonesia.

Abstract | Follicular cysts are important ovarian disorders in dairy cattle because persistent anovulatory follicles delay conception, prolong days open, increase culling risk, and consequently reduce milk-production efficiency. Although follicular cysts are commonly regarded as ovarian lesions, their development is linked to endocrine, inflammatory, metabolic, and liver-associated metabolic disturbances. This exploratory comparative study aimed to compare serum SDS-PAGE protein profiles and alanine aminotransferase (ALT) activity between estradiol valerate (EV)- and testosterone propionate (TP)-induced follicular cyst-like rat models. Thirty adults female Wistar rats (*Rattus norvegicus*) were randomly allocated into two induced model groups (n = 15/group). Follicular cyst-like conditions were induced using EV (2 mg/kg BW, intraperitoneally, for 2 days) or TP (100 mg/kg BW, intraperitoneally, for 12 days). Model confirmation was based primarily on vaginal cytology, while gross morphology was interpreted only as supportive observation. Serum samples were analyzed using sodium dodecyl sulfate-polyacrylamide gel electrophoresis (SDS-PAGE) for exploratory protein profiling and enzyme-linked immunosorbent assay (ELISA) for ALT quantification. Both hormone-induced groups showed broadly similar SDS-PAGE serum protein distribution patterns, with dominant bands at 66-70 kDa, 75-80 kDa, and 50-56 kDa. A qualitatively stronger 50-56 kDa region was observed in the TP-induced group; however, this observation should be interpreted as preliminary because protein identity and band-intensity differences were not confirmed by protein-specific assays. The TP group showed a numerically higher ALT concentration than the EV group (10.37 +/- 0.16 U/L vs. 8.65 +/- 0.07 U/L), but the difference was not statistically significant ($p > 0.05$). EV- and TP-induced follicular cyst-like rat models showed broadly similar exploratory serum protein profiles, with a preliminary qualitative difference in the 50-56 kDa region in the TP group. These findings may guide future targeted validation studies but do not establish definitive protein identity, liver pathology, clinical biomarkers, or immediate clinical application in livestock reproductive health management.

Keywords | Cystic ovarian disease, Serum protein profiling, SDS-PAGE, Alanine aminotransferase, Estradiol valerate, Testosterone propionate, Rat model

Received | June 05, 2026; **Accepted** | July 10, 2026; **Published** | July 28, 2026
***Correspondence** | Yudit Oktanella, Department of Veterinary Reproduction, Faculty of Veterinary Medicine, Universitas Brawijaya, Puncak Dieng Eksklusif, Kalisongo, Dau, Malang, East Java 65151, Indonesia; **Email:** yudito@ub.ac.id
Citation | Oktanella Y, Mahalita NR, Ismiawati H, Prastiya RA (2026). Serum protein and ALT profiles in hormone-induced follicular cyst rat models. Adv. Anim. Vet. Sci., 14(8):1595-1604.
DOI | https://dx.doi.org/10.17582/journal.aavs/2026/14.8.1595.1604
ISSN (Online) | 2307-8316

INTRODUCTION

Follicular cysts are common ovarian disorders among dairy cows, and their contribution to reproductive failure is important. Long-term anovulatory follicles disrupt oestrous cyclicity, lengthen days open, decrease conception rate, and escalate treatment costs; moreover, they can indirectly decrease milk production efficiency

by further delaying pregnancy and lengthening non-productive periods (Borş *et al*., 2018; Borş and Borş, 2020; Lysenko *et al*., 2024). As such, follicular cysts should be regarded not only as ovarian disease but also as herd-level disease, due to their direct or indirect impact on reproductive and production performance.

The pathology of follicular cysts involves permanent dominant follicles that do not regress and do not have a functional corpus luteum. Ovarian changes can show marked enlargement and fluid filling, although small cell structures may be diminished or absent, as well as fine-to-medium changes such as thinning of the granulosa cell layer, altered theca cell function, reduced or absent corpora lutea, and follicular persistence or atresia. Their pathogenesis is thought to be due to hypothalamic-pituitary-ovarian axis signals, disrupted luteinizing hormone release, abnormal steroidogenesis, oxidative stress, and dysregulation of inflammation. Control and treatment in cattle are typically hormonal protocols based on the cyst class (GnRH, hCG, or prostaglandin-based regimens) with improved metabolic, nutritional, and herd-management risk factors (Borş *et al*., 2018; Borş and Borş, 2020).

Recent investigations demonstrate that cystic ovarian disease is more than mere local ovarian morphology. Steroidogenic gene alterations, such as STAR, 3β-HSD, CYP11A1, and CYP17A1, have been implicated in the prevalence of bovine ovarian follicular cysts (Xu *et al*., 2023). In addition, inflammatory and acute-phase proteins, TNF-alpha, IL-6, IL-10, haptoglobin, and serum amyloid A, are implicated in cystic ovarian disease of dairy cows (Brodzki *et al*., 2019). These alterations help illustrate the systemic sequelae of follicular cysts via inflammatory activation, hepatic acute-phase protein production, oxidative stress and metabolic modification. Steroid-hormone metabolism, regulation of insulin-like growth factors, lipid and glucose homeostasis, and synthesis of serum proteins are closely linked to hepatic reproductive function. Therefore, ovarian endocrine disturbance can affect hepatometabolic pathways and liver-derived serum biomarkers (Rhyu and Yu, 2021).

Alanine aminotransferase (ALT) is a common hepatocellular biomarker that should be interpreted cautiously, as circulating ALT may reflect multiple mechanisms, including frank hepatocyte necrosis (McGill, 2016; Smith *et al*., 2020). Due to the challenge of studying naturally occurring follicular cysts in large livestock in controlled experimental conditions, hormonally induced rodent models are ideal candidates for translation. Oestradiol valerate and testosterone propionate models replicate several features associated to follicular persistence, anovulation, disrupted cyclicity, cyst-like ovarian shape, and endocrine disturbance, but no rodent model fully recapitulates spontaneous bovine cystic ovarian disease (Ryu *et al*., 2019; Kamada *et al*., 2021; Esan *et al*., 2023; Hu *et al*., 2024).

For instance, serum protein profiling by SDS-PAGE provides an inexpensive first-line means of assessing broad-spectrum systemic alterations in transport proteins, acute-phase proteins, immunoglobulin-related fractions, and liver-derived protein subdomains. In contrast, one-dimensional SDS-PAGE screens proteins only by apparent molecular weight and therefore cannot determine definitive protein localization. Such band assignments should therefore be considered putative and must ultimately be validated by Western blotting, protein-specific ELISA or LC-MS/MS. The novelty and originality of this study were achieved through integrated exploratory SDS-PAGE serum protein profiling and ALT ELISA to assess systemic inflammatory and hepatometabolic responses in hormone-induced follicular cyst rats. This technique could aid in identifying candidate serum biomarker regions for later validation in dairy animals. Based on these details, this study sought to correlate serum protein profiles and ALT concentrations between EV- and TP- induced follicular cyst rat models. We hypothesized that induction of cystic follicles changes protein band patterns in serum and ALT levels, indicating systemic rather than localized ovarian pathology.

MATERIALS AND METHODS

Animals and experimental design

The study was conducted in the laboratory animal and veterinary reproduction research facilities of the Faculty of Veterinary Medicine, Universitas Brawijaya, Malang, Indonesia. The study used a controlled exploratory comparative design to compare two hormone-induced follicular cyst-like models: An EV-induced group and a TP-induced group. A total of 30 adult female Wistar rats (*Rattus norvegicus*) aged 10 weeks and weighing approximately 120 g were acclimatized for 7 days under a 12 h light/12 h dark cycle, controlled temperature and humidity, standard pellet diet, and water ad libitum. The age of 10 weeks was selected because female rats at this stage are sexually mature while still minimizing age-related reproductive variability. After acclimatization, rats were assigned to the two experimental groups using simple random allocation (n= 15/group). SDS-PAGE and ELISA analyses were performed using coded samples where possible; complete blinding during all outcome assessments was not feasible and is acknowledged as a limitation. A schematic overview of the experimental design is presented in Figure 1.

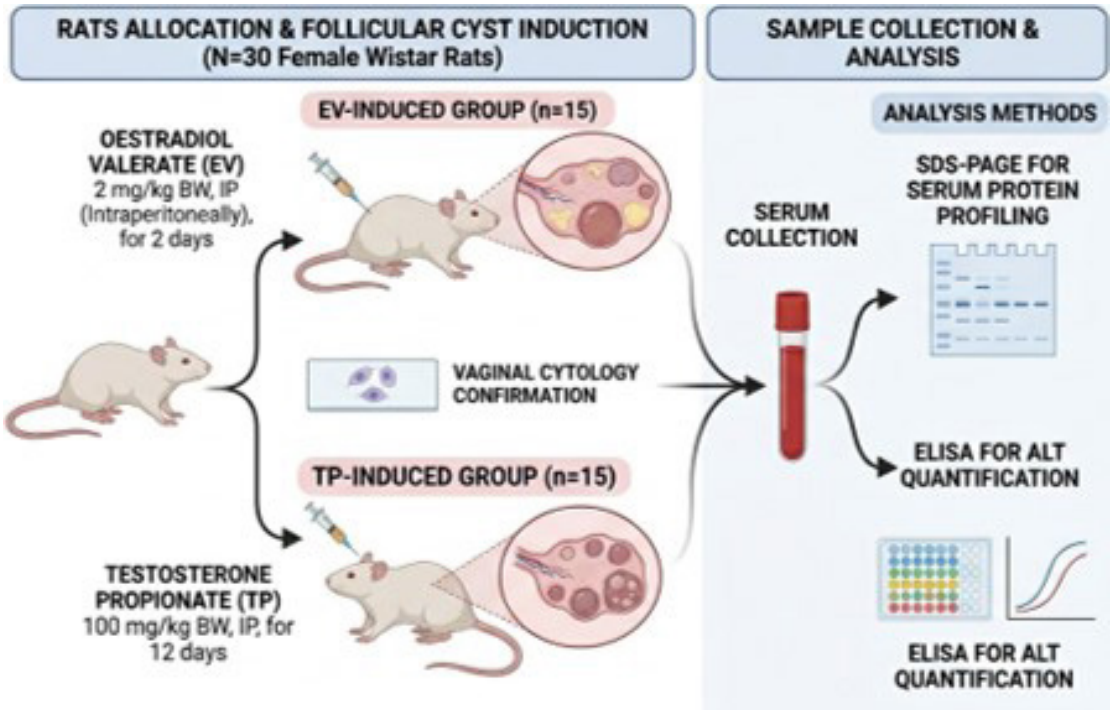

Figure 1: Schematic overview of the experimental design.

Cystic follicle model induction and confirmation

The follicular cyst-like model was induced using testosterone propionate (TP) and estradiol valerate (EV), adapting established protocols known to replicate PCOS-like reproductive abnormalities, including anovulation, disrupted cyclicity, and cyst-like ovarian changes (Espinoza *et al*., 2018; Hu *et al*., 2024; Venegas *et al*., 2019). Rats in the TP group received intraperitoneal injections of testosterone propionate (Sigma-Aldrich, USA) at a dose of 100 mg/kg BW for 12 days. Rats in the EV group received estradiol valerate (Java Animal Care, Indonesia) dissolved in sterile pharmaceutical-grade sesame oil (Brataco Chemika, Indonesia) at a dose of 2 mg/kg BW intraperitoneally for 2 days. These induction protocols differ in dose, duration, and handling frequency because EV and TP induce reproductive abnormalities through different endocrine mechanisms; therefore, the comparison reflects model-specific responses rather than identical hormone-exposure conditions. The intraperitoneal route was used to support consistent systemic hormone delivery, but this route does not fully mimic physiological hormone exposure in naturally occurring livestock disease.

Successful model establishment was confirmed post-induction via vaginal cytology. Vaginal smears were collected for two consecutive days every six hours using sterile cotton swabs moistened with 0.9% NaCl. The collected vaginal cells were gently rolled onto clean glass slides, air-dried, stained with Giemsa, and examined under a light microscope. Oestrous cycle stages were determined based on the predominant cell populations in the smear: nucleated epithelial cells for proestrus, cornified epithelial cells for oestrus, mixed epithelial cells and leukocytes for metestrus, and predominant leukocytes for dioestrus, following standard criteria for evaluating rodent oestrous cyclicity (Ajayi and Akhigbe, 2020; Kamada *et al*., 2021). Rats were considered positive for the cystic follicle model when vaginal smears showed persistent oestrus, characterized by continuous predominance of cornified epithelial cells during two consecutive days of observation. Where applicable, ovarian morphology, including the presence of enlarged cystic follicles, reduced granulosa cell layers, and reduced or absent corpora lutea, was further assessed to support model confirmation, consistent with the histological criteria reported in oestradiol valerate-induced PCOS-like rats (Espinoza *et al*., 2018).

Clinical monitoring and gross examination

Animals were monitored during induction for general condition, behavior, feed intake, injection-site reaction, and visible distress. At terminal sampling, ovaries were inspected visually during necropsy to support interpretation of systemic findings (Figure 2).

Although EV and TP induction were intended to establish follicular cyst model rats, the gross ovarian morphology in the representative images did not show prominent or well-demarcated cyst-like follicles in either group. Only small suspected follicular structures were observed, and no significant macroscopic follicular cyst formation was evident. Therefore, confirmation of cystic follicle development requires microscopic or histopathological evaluation.

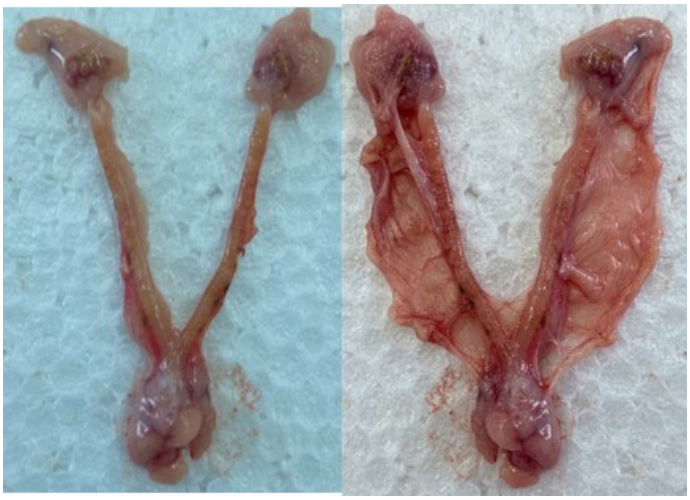

Figure 2: Representative gross morphology of the reproductive tract and ovaries from rats induced with estradiol valerate/EV (left) for 2 days and testosterone propionate/TP for 12 days (right). The ovaries are located at the cranial ends of the uterine horns.

Collection and preparation of serum

At the conclusion of the experiment, rats were fasted for 8-12 h to reduce metabolic fluctuation before serum biochemical analysis. Animals were deeply anesthetized by intraperitoneal administration of ketamine hydrochloride (80 mg/kg BW) and xylazine hydrochloride (10 mg/kg BW). Blood samples were collected by terminal cardiac puncture into plain sterile tubes to obtain sufficient serum volume for SDS-PAGE and ELISA analyses, after which rats were euthanized by cervical dislocation while still under deep anaesthesia. Blood samples were allowed to clot at room temperature for 20-30 min. Serum was separated by centrifugation at 3000 rpm for 10-15 min at 4°C, transferred to sterile microtubes, and stored at -80°C until SDS-PAGE and ALT analysis. Repeated freeze-thaw cycles were avoided to preserve serum protein integrity. Samples were visually checked for gross haemolysis before analysis, and serum integrity is acknowledged as important for interpreting both protein-band patterns and ALT activity.

Serum protein profiling using SDS-PAGE

Serum protein characteristics were determined by sodium dodecyl sulfate–polyacrylamide gel electrophoresis (SDS-PAGE). Electrophoresis equipment and primary reagents, including the PowerPac power supply, molecular weight markers, Laemmli sample buffer, and staining reagents, were sourced from Bio-Rad Laboratories (USA).

Before electrophoresis, crude serum protein concentration was measured spectrophotometrically using the Bradford method. A standard curve was generated using bovine serum albumin at predefined concentrations of 0, 0.125, 0.250, 0.500, 0.750, 1.000, 1.500, and 2.000 mg/mL. Because baseline crude serum protein concentrations usually ranged from 60 to 85 mg/mL, samples were diluted 1:50 to 1:100 with distilled water or phosphate-buffered saline to maintain absorbance values within the linear assay range. After incubation for 5-10 min at room temperature, absorbance was measured at 595 nm, and all samples were normalized to 2.0 mg/mL.

For electrophoresis, 10 µL of each normalized sample, corresponding to 20 µg protein per lane, was mixed with 4x Laemmli sample buffer containing beta-mercaptoethanol at a 3:1 ratio. Mixtures were heated at 95°C for 5 min and briefly centrifuged. Proteins were separated using a Mini-PROTEAN Tetra Cell system on hand-cast polyacrylamide gels comprising a 12% resolving gel and a 4% stacking gel. Electrophoresis was performed in 1x Tris-glycine-SDS running buffer at 80 V through the stacking gel and 120 V through the resolving gel until the dye front reached the bottom.

Gels were stained with Coomassie Brilliant Blue R-250 and destained until clear bands were visible. Gel images were captured using a Gel Doc imaging system. Band detection, apparent molecular-weight estimation, and descriptive densitometric assessment were performed using Image Lab software, with band intensity scaled to total lane density to reduce loading variation. Because one-dimensional SDS-PAGE provides only apparent molecular-weight separation, all band identities were interpreted as putative molecular-weight regions and require confirmation by Western blotting, protein-specific ELISA, or LC-MS/MS. Band-intensity observations were used only for descriptive qualitative comparison and were not subjected to inferential statistical testing.

ALT ELISA

Serum ALT concentrations were quantified using a commercial Rat ALT/GPT ELISA Kit (Bioassay Technology Laboratory, Shanghai, China) according to the manufacturer's protocol. Samples, standards, and blanks were analyzed in duplicate using a quantitative sandwich ELISA format. After incubation, washing, addition of detection reagents, and chromogenic reaction development, optical density was measured at 450 nm using an iMark Microplate Absorbance Reader (Bio-Rad Laboratories, USA). Final ALT concentrations were calculated from the standard curve. ALT was interpreted as a complementary hepatocellular and hepatometabolic biomarker, recognizing that ALT elevation may occur through multiple biological mechanisms and is not solely specific for hepatocyte necrosis (McGill, 2016; Smith *et al.*, 2020).

Statistical analysis

Statistical analyses were performed using IBM SPSS Statistics for Windows, Version 29.0 (IBM Corp., Armonk, NY, USA). Quantitative data are expressed as the mean ±

standard deviation (SD). The normality of data distribution and the homogeneity of variances were assessed using the Shapiro–Wilk and Levene's tests, respectively. Statistical comparisons between the oestradiol valerate (EV) and testosterone propionate (TP) groups were conducted using an independent-samples *t*-test for normally distributed data. If the data violated the assumption of normality, the Mann–Whitney U test was applied. Differences were considered statistically significant at $p < 0.05$. SDS-PAGE profiles were evaluated descriptively based on apparent molecular weight and relative band intensity.

RESULTS

Clinical observation, mortality record, and gross findings

Clinical observation was used to monitor the general condition of rats during model induction. Clinical monitoring was qualitative and included general condition, visible distress, visible feed intake, and injection-site reactions. No quantitative clinical-score dataset, complete mortality log, serial body-weight dataset, or systematic gross-lesion scoring sheet was available in the submitted manuscript file; therefore, these endpoints were not subjected to statistical analysis. The interpretation of the present study was consequently focused on vaginal cytology confirmation, serum SDS-PAGE patterns, and ALT concentration.

Based on the available gross images (Figure 2), both groups showed visible reproductive tract structures, including the uterine horns and ovaries located at the cranial ends of the uterine horns. However, prominent, well-demarcated, enlarged, translucent, fluid-filled follicular cysts were not clearly observed in either the EV- or TP-induced group. Only small suspected follicular structures could be grossly identified, and no significant macroscopic cyst-like ovarian enlargement was evident.

These findings indicate that, although EV and TP induction were used to establish follicular cyst-like rat models, the presence of follicular cysts could not be confirmed by gross morphology alone in the representative images. Therefore, cystic follicle development should be interpreted cautiously and should be confirmed in future studies by ovarian histopathology, together with vaginal cytology and supporting biochemical or molecular findings. The lack of clear gross cystic changes is acknowledged as a limitation of macroscopic assessment in the present study.

SDS-PAGE serum protein profile

The SDS-PAGE profile of serum proteins was derived from the rat oestradiol valerate (EV) and testosterone propionate (TP) induced follicular cysts. Following spectrophotometric normalization of all samples to a common protein concentration, numerous serum protein bands spanning a wide molecular weight range were visualized on the gel. The predominant band was observed in the 66–70 kDa range, presumably corresponding to serum albumin. Additional protein bands were observed at approximately 75–80 kDa, 50–56 kDa, 41–45 kDa, 35–40 kDa, 28–30 kDa, and 25 kDa (Figure 3).

Based on their apparent molecular weights and known serum protein distributions, these bands were interpreted only as putative molecular-weight regions that may overlap with transferrin-related, albumin-like, α1-antitrypsin/ALT-related, α1-acid glycoprotein-related, haptoglobin-related, apolipoprotein A-I-related, and immunoglobulin light-chain-related regions (Table 1). These assignments are preliminary and require validation by Western blotting, protein-specific ELISA, or LC-MS/MS.

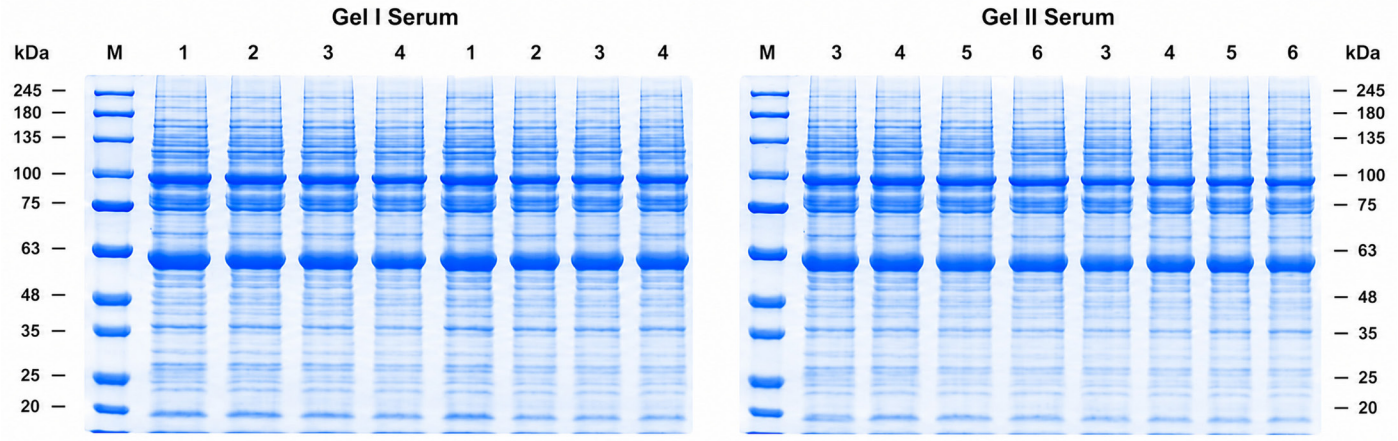

Figure 3: SDS-PAGE profile of serum proteins in hormone-induced follicular cyst-like rat models. The left panel (Gel I) shows serum protein bands from the TP-induced group, whereas the right panel (Gel II) shows serum protein bands from the EV-induced group. M: molecular-weight marker; lanes 1-4 (Gel I) and lanes 3-6 (Gel II) represent serum samples from the experimental animals, loaded in duplicate. Because the groups are shown on separate gel panels, band-intensity comparison should be interpreted cautiously and descriptively only.

Table 1: Putative serum protein bands detected by SDS-PAGE.

Approximate molecular weight	Putative protein candidate	Biological relevance
120–132 kDa	Transferrin-related region	Oxidative stress and inflammatory response
75–80 kDa	Albumin-like region	Iron transport and metabolic regulation
66–70 kDa	α1-antitrypsin/ALT-related or overlapping serum protein region	Major serum transport protein and liver-derived protein
50–56 kDa	α1-acid glycoprotein-related region	Inflammation, immune response, and hepatocellular involvement
41–45 kDa	Haptoglobin-associated or overlapping serum protein region	Acute-phase and inflammatory response
35–40 kDa	Apolipoprotein A-I-related region	Acute-phase response and oxidative stress
28–30 kDa	Immunoglobulin light-chain-related region	Lipid metabolism and systemic metabolic disturbance
±25 kDa	Transferrin-related region	Humoral immune response

Note: All protein assignments are based only on apparent molecular weight in one-dimensional SDS-PAGE and require confirmation by Western blotting, protein-specific ELISA, or LC-MS/MS.

Table 2: Serum ALT levels in EV- and TP-induced follicular cyst model rats.

Group	ALT concentration (U/L), mean ± SD	Statistical interpretation
EV-induced follicular cyst-like model	8.65 ± 0.07	Reference induced-model comparison group
TP-induced follicular cyst-like model	10.37 ± 0.16	Numerically higher than EV, but not statistically significant ($p > 0.05$)

Note: Values are presented as mean ± SD based on the available manuscript dataset. The non-significant ALT result should not be interpreted as confirmed liver injury or hepatic-metabolic dysfunction.

A qualitative comparison between the EV and TP groups demonstrated broadly similar overall serum protein distribution patterns, with both groups exhibiting predominantly albumin-like and lower-molecular-weight regions. The TP group displayed a visibly stronger band in the approximately 50-56 kDa region compared with the EV group. However, no statistical comparison of band intensity was performed, and this qualitative observation should not be interpreted as confirmed differential protein expression.

Serum ALT levels and integrated protein profile analysis

Serum ALT levels were evaluated as a complementary liver-associated biochemical marker. The mean ALT level was 8.65 ± 0.07 U/L in the EV group and 10.37 ± 0.16 U/L in the TP group (Table 2). Although the TP group showed a numerically higher ALT value, this difference was not statistically significant ($p > 0.05$) and therefore cannot be interpreted as evidence of confirmed hepatocellular injury or hepatic-metabolic dysfunction. The ELISA assay demonstrated strong standard-curve linearity (R^2 = 0.9913).

Overall, the TP group showed a qualitatively stronger 50-56 kDa molecular-weight region and a numerically higher ALT concentration. These findings should be interpreted as preliminary and hypothesis-generating only. They do not establish definitive protein identity, quantitative differential protein expression, liver pathology, or confirmed systemic biomarkers without additional histological, biochemical, and protein-specific validation.

DISCUSSION

In the current study, sera derived from estradiol valerate (EV)- and testosterone propionate (TP)-induced follicular cyst-like rat models showed broadly similar exploratory SDS-PAGE protein profiles, with dominant molecular-weight regions at 66-70 kDa, 75-80 kDa, and 50-56 kDa. These data suggest that, despite their distinct endocrine mechanisms, both hormonal induction methods may yield the same broad distribution patterns of serum proteins. Nevertheless, the present design does not comprise a healthy, non-induced control group, nor do the data allow determination of whether, on the basis of this hormone induction, serum protein patterns or ALT activity were altered compared to physiological normal. Cystic ovarian diseases in dairy cows have the potential to cause systemic steroidogenic, metabolic, and immunological alterations, thereby warranting careful exploration of serum-specific variation in reproductive diseases (Lima *et al.*, 2019). Anovulation, continued follicular development, and steroid imbalance are well documented in the laboratory as hallmarks of ovarian cyst formation in hormonally induced rat models (Morales-Ledesma *et al.*, 2017).

Indeed, the predominant 66-70 kDa region in both the EV and TP groups is closest to the albumin-type molecular-weight region, with albumin constituting the largest liver-derived serum protein and being essential for transport, maintenance of oncotic pressure, and antioxidant buffering. However, SDS-PAGE alone cannot confirm albumin identity. Rajala (2008) also noted favorable conditions for serum proteomic electrophoresis and found that electrophoretic screening is an effective way to assess the serum proteins. In livestock, metabolic and hepatic status are well associated with reproductive performance, and bovine ovarian follicular cysts are associated with endocrine-metabolic disturbances and alterations in steroidogenesis-related genes, such as STAR, 3β-HSD, CYP11A1, and CYP17A1 (Xu *et al*., 2023). Cattaneo *et al*. (2021) also reported that albumin-associated indices, namely the albumin-to-globulin ratio, were predictors of inflammatory and metabolic status in dairy cows. The strong albumin-like region identified in the current rat model could be considered a candidate serum region for further validation rather than for demonstrating established hepatic or reproductive biomarker action. Biologically relevant protein bands are also in the 35- 60 kDa region, but they are not as clear. This large region may contain overlapping acute-phase proteins, immunoglobulin fragments, α1-antitrypsin proteins, haptoglobin-associated fractions, and other inflammation-related serum proteins (Zhang *et al*., 2021; Hashimoto *et al*., 2024). Brodzki *et al*. (2019) report altered serum cytokines and acute-phase proteins (TNF-α, IL-6, IL-10, haptoglobin, serum amyloid A) from dairy cows having cystic ovarian disease. Likewise, DIA-based proteomics (Yu *et al*., 2021) had identified inflammation-, oxidative stress-, and cellular regulation-related serum proteins in women with PCOS. While cystic ovarian disease in cows and PCOS in women are separate disorders, we speculate that both present with endocrine dysregulation, follicular persistence, and a systemic inflammatory response. Accordingly, these SDS-PAGE bands could be classified as candidate molecular-weight regions that need protein-specific validation.

Protein bands in the 35–60 kDa region may also have biological significance, as they may contain acute-phase proteins, immunoglobulin fragments, α1-antitrypsin-related proteins, haptoglobin-associated fractions, and other inflammation-associated serum proteins (Zhang *et al*., 2021; Hashimoto *et al*., 2024). This band pattern is consistent with the results of Brodzki *et al*. (2019), who observed abnormal serum cytokines and acute-phase proteins, primarily TNF-α, IL-6, IL-10, haptoglobin, and serum amyloid A, in dairy cows with cystic ovarian disease. These results suggest that inflammation plays a role in the pathophysiology of ovarian cyst development. The same systemic inflammatory and oxidative patterns have been described in women with polycystic ovary syndrome as well. Yu *et al*. (2021) used DIA-based proteomics to identify 80 differentially expressed serum proteins in women with PCOS, most of which were associated with inflammation, oxidative stress, and cellular regulation. Cystic ovarian disease in cows and PCOS in women are distinct clinical conditions, but they share endocrine dysregulation, follicular persistence, and systemic inflammation.

An integrative analysis of the role of immune-system processes in complement dysregulation in PCOS also confirms a possible role for immune-mediated serum pathways. Luan *et al*. (2022) described changes in immune regulation in PCOS, and Butler *et al*. (2022) demonstrated that multiple components of the complement cascade correlated with obesity, hyperandrogenaemia, and insulin resistance in women with PCOS. The present study was unrelated to complement proteins and did not employ LC-MS/MS, Western blotting, or protein-specific ELISA. Thus, any sense-making of immune-related bands is still tentative. The presence of multiple middle-to-high molecular weight regions suggests that hormonally induced follicular cyst-like models may encompass candidate immunometabolic serum regions that warrant priority for future targeted validation.

A salient descriptive difference of interest between the 2 induction models was the qualitatively stronger (50-56 kDa) region in the TP group. This molecular-weight region might harbour a high degree of homogenization of serum proteins, e.g., the α1-antitrypsin fraction, immunoglobulin fragments, transthyretin-associated variants, or liver-related enzyme sections; however, the allocation of these is not yet definitive. The ALT in the TP group in this study was numerically higher than in the EV group, but this difference was not significant. Accordingly, the ALT value should not connote evidence of established hepatocellular injury, liver impairment, or clinically relevant hepatic metabolism disorders. Serum ALT should not be seen as a passive marker of hepatocellular necrosis; McGill (2016) proposed that, even though Smith *et al*. (2020) presented more comprehensive mechanisms of ALT release by impaired or hyperregulatory hepatocytes. Because oxidative stress is relevant to reproductive disorders, the numerical ALT trend might reflect a preliminary exposure to endocrine-metabolic stress, but this interpretation is speculative without validation of AST, bilirubin, liver histopathology, and protein markers (Smith *et al*., 2020; Aitken *et al*., 2022; Rautela *et al*., 2021).

The differences between the EV and TP groups also mirror divergent protocols toward endocrine induction. Espinoza *et al*. (2018) injected EVs in rats, which elicited PCOS symptoms such as polycystic ovaries and ovarian anovulation, hyperandrogenism, and these responses

may reflect ovarian sympathetic responses. TP induces androgen excess and has differential effects on reproductive dysfunction from EVs. Hu *et al.* (2024) reported differences in reproductive phenotypes and metabolic traits in PCOS rats following treatment with letrozole, testosterone propionate, and a high-fat diet. These findings are consistent with the cautious interpretation that the TP-treated rats had a qualitatively stronger 50-56 kDa region and numerically higher ALT concentration than the EV-treated rats. However, the duration and frequency of administration will vary between TP and EV protocols, and so the current comparison reflects model-specific differences rather than equivalent hormonal experience.

In general, this result supports the rationale for investigating SDS-PAGE as a means of identifying wide-spectrum serum proteins in hormonally induced follicular cyst-like rat models. Protein assignments in this study are presumptive, as SDS-PAGE separates proteins based on apparent molecular weight and cannot identify specific proteins. As such, the bands observed at approximately 66-70 kDa, 75-80 kDa, and 50-56 kDa should be considered candidate molecular-weight regions rather than reported positive biomarkers. Western blotting, protein-specific ELISA or LC-MS/MS, as well as correlation with ovarian histopathology and with liver-associated biochemical panels and reproductive outcomes, are required for further confirmation.

Study limitations

The present study has several limitations. First, a healthy, non-induced control group was not included, so the study cannot determine whether EV or TP induction altered serum protein patterns or ALT activity relative to baseline physiology. Second, gross ovarian morphology did not clearly confirm the presence of prominent cyst-like follicles, and ovarian histopathology was not performed. Third, one-dimensional SDS-PAGE cannot identify specific proteins, and no Western blotting, protein-specific ELISA, or LC-MS/MS validation was performed. Fourth, complete clinical-score, mortality, serial body weight, exact cytological success-count, haemolysis-exclusion, assay-performance, and effect-size datasets were not available in the submitted manuscript file. These limitations restrict the interpretation of the findings to exploratory, descriptive, and hypothesis-generating observations.

Recommendations and future directions

Future studies should include a healthy non-induced control group, formal sample-size calculation, longitudinal clinical observation, mortality recording, serial body-weight monitoring, gross ovarian photographs, ovarian histopathology, and additional liver-associated biomarkers such as AST and bilirubin. Protein bands of interest, especially the 50-56 kDa region, should be validated by Western blotting, protein-specific ELISA, or LC-MS/MS. Validation in dairy cattle with naturally occurring follicular cysts is recommended before clinical application in livestock reproductive health management.

CONCLUSION

EV- and TP-induced follicular cyst-like rat models showed broadly similar exploratory SDS-PAGE serum protein profiles, with a qualitative difference at 50–56 kDa observed in the TP group. The TP group also showed a numerically higher ALT concentration, although this difference was not statistically significant. Therefore, these findings should be interpreted as preliminary and hypothesis-generating only, rather than as evidence of confirmed differential protein expression, liver pathology, or validated systemic biomarkers. Further validation using ovarian histopathology, additional liver-associated biochemical markers, and protein-specific identification methods is required before these candidate findings can be applied to livestock reproductive health management.

Data availability

The datasets generated and analyzed during the current study are available from the corresponding author upon reasonable request.

ACKNOWLEDGEMENTS

The authors would like to thank the Faculty of Veterinary Medicine, Universitas Brawijaya, for providing the laboratory facilities and technical support necessary for this study. We also extend our gratitude to the research assistants who assisted in animal handling, tissue processing, and the execution of biochemical assays.

NOVELTY STATEMENT

This study provides an exploratory comparison of SDS-PAGE serum protein profiles and ALT activity between EV- and TP-induced follicular cyst-like rat models. The novelty lies in identifying candidate serum molecular-weight regions, particularly the qualitative 50-56 kDa region in the TP group, for future targeted validation. The findings do not establish definitive protein identity, liver pathology, or clinical biomarkers, but they may help guide subsequent protein-specific and livestock-based studies.

AUTHOR'S CONTRIBUTION

YO: conceptualization, methodology, data collection, formal analysis, and manuscript drafting. NRM: data interpretation, and manuscript drafting. HI: methodology

support, data analysis, and manuscript review. RAP: manuscript review and editing. All authors have read and approved the final version of the manuscript.

Ethical statement

All experimental procedures were approved by the Animal Ethics Committee of Universitas Brawijaya under ethical clearance number 090-KEP-UB-2022. The experimental protocol followed institutional animal ethics standards and was reported in accordance with the ARRIVE 2.0 recommendations for in vivo studies, including ethical approval, randomization, transparent group allocation, and clear reporting of sample processing and outcome measurements (Percie du Sert *et al*., 2020).

Abbreviation

ALT, Alanine aminotransferase; BW, Body weight; ELISA, Enzyme-linked immunosorbent assay; EV, Estradiol valerate; FC, Follicular cyst; HPO axis, Hypothalamic-pituitary-ovarian axis; IP, Intraperitoneal; OD, Optical density; PCOS, Polycystic ovary syndrome; SDS-PAGE, Sodium dodecyl sulfate-polyacrylamide gel electrophoresis; TP, Testosterone propionate.

Generative AI and AI assisted technology statement

The authors acknowledge that AI-assisted language tools were used solely to support language editing, sentence clarity, and grammar improvement. The scientific content, experimental data, interpretation, conclusions, and final approval of the manuscript remain the sole responsibility of the authors.

Conflict of interest

The authors have declared no conflict of interest.

REFERENCES

Aitken RJ, Bromfield EG, Gibb Z (2022). Oxidative stress and reproductive function: The impact of oxidative stress on reproduction: A focus on gametogenesis and fertilization. Reproduction, 164(6): F79-F94. https://doi.org/10.1530/REP-22-0126

Ajayi AF, Akhigbe RE (2020). Staging of the estrous cycle and induction of estrus in experimental rodents: An update. Fertil. Res. Pract., 6: 5. https://doi.org/10.1186/s40738-020-00074-3

Borş SI, Borş A (2020). Ovarian cysts, an anovulatory condition in dairy cattle. J. Vet. Med. Sci., 82(10): 1515-1522. https://doi.org/10.1292/jvms.20-0381

Borş SI, Ibănescu I, Creangă Ş, Borş A (2018). Reproductive performance in dairy cows with cystic ovarian disease after single treatment with buserelin acetate or dinoprost. J. Vet. Med. Sci., 80(7): 1190-1194. https://doi.org/10.1292/jvms.17-0690

Brodzki P, Brodzki A, Krakowski L, Dąbrowski R, Szczubiła M, Bochniarz M (2019). Levels of selected cytokines and acute-phase proteins in the serum of dairy cows with cystic ovarian disease. Theriogenology, 123: 20-25. https://doi.org/10.1016/j.rvsc.2018.12.007

Butler AE, Moin ASM, Sathyapalan T, Atkin SL (2022). Components of the complement cascade differ in polycystic ovary syndrome. Int. J. Mol. Sci., 23(20): 12232. https://doi.org/10.3390/ijms232012232

Cattaneo L, Lopreiato V, Piccioli-Cappelli F, Trevisi E, Minuti A (2021). Plasma albumin-to-globulin ratio before dry-off as a possible index of inflammatory status and performance in the subsequent lactation in dairy cows. J. Dairy Sci., 104(7): 8228-8242. https://doi.org/10.3168/jds.2020-19944

Esan WS, Akintayo CO, Sanya O, Oluwaseun OA, Olubayo G, Adelekan AL (2023). Induction and treatment of polycystic ovary syndrome with plant extract in rats: A systematic review. Eur. J. Med. Plants, 34(2): 34-48. https://doi.org/10.9734/ejmp/2023/v34i21124

Espinoza JA, Alvarado W, Venegas B, Domínguez R, Morales-Ledesma L (2018). Pharmacological sympathetic denervation prevents the development of polycystic ovarian syndrome in rats injected with estradiol valerate. Reprod. Biol. Endocrinol., 16: 86. https://doi.org/10.1186/s12958-018-0400-8

Hashimoto H, Okazaki T, Honkura Y, Ren Y, Ngamsnae P, Hisaoka T, Koshiba Y, Suzuki J, Ebihara S, Katori Y (2024). Nrf2 deficiency exacerbates the decline in swallowing and respiratory muscle mass and function in mice with aspiration pneumonia. Int. J. Mol. Sci., 25(21): 11829. https://doi.org/10.3390/ijms252111829

Hu R, Huang Y, Liu Z, Dong H, Ma W, Song K (2024). Characteristics of polycystic ovary syndrome rat models induced by letrozole, testosterone propionate and high-fat diets. Reprod. Biomed. Online, 50: 104296. https://doi.org/10.1016/j.rbmo.2024.104296

Kamada S, Yamamoto Y, Aoki H, Tamura K, Takeda A, Minato S (2021). A novel PCOS rat model and an evaluation of its reproductive, metabolic, and behavioral phenotypes. Reprod. Med. Biol., 21: e12416. https://doi.org/10.1002/rmb2.12416

Lima FS, Acosta DAV, Egan TR, Skenandore C, Sulzberger S, French DD, Cardoso FC (2019). Steroidogenic, metabolic, and immunological markers in dairy cows diagnosed with cystic ovarian follicles at early and mid-late lactation. Front. Vet. Sci., 6: 324. https://doi.org/10.3389/fvets.2019.00324

Luan Y, Zhang L, Peng Y, Li Y, Liu R, Yin C (2022). Immune regulation in polycystic ovary syndrome. Clin. Chim. Acta, 531: 265-272. https://doi.org/10.1016/j.cca.2022.04.234

Lysenko AV, Mihkalev VI, Safonov VA, Sineva AM (2024). Ovarian dysfunction in cows and its distribution in black soil farms. BIO Web Conf., 95: 01031. https://doi.org/10.1051/bioconf/20249501031

McGill MR (2016). The past and present of serum aminotransferases and the future of liver injury biomarkers. Excli J., 15: 817-828.

Morales-Ledesma L, Díaz Ramos JA, Trujillo Hernández A (2017). Polycystic ovary syndrome induced by exposure to testosterone propionate and effects of sympathectomy on the persistence of the syndrome. Reprod. Biol. Endocrinol., 15(1): 50. https://doi.org/10.1186/s12958-017-0267-0

Percie du Sert N, Hurst V, Ahluwalia A, Alam S, Avey MT, Baker M (2020). The ARRIVE guidelines 2.0: Updated guidelines for reporting animal research. PLoS Biol., 18(7): e3000410.

https://doi.org/10.1371/journal.pbio.3000410

Rajala RVS (2008). The optimized conditions of two-dimensional polyacrylamide gel electrophoresis for serum proteomics. J. Proteomics Bioinform., 1(5): 1-8.

Rautela R, Katiyar R, Deori S, Singh M (2021). Does oxidative stress impact bovine reproductive disorders. Indian J. Anim. Reprod., 42(2): 1-7.

Rhyu J, Yu R (2021). Newly discovered endocrine functions of the liver. World J. Hepatol., 13(11): 1611. https://doi.org/10.4254/wjh.v13.i11.1611

Ryu Y, Kim SW, Kim YY, Ku SY (2019). Animal models for human polycystic ovary syndrome (PCOS) focused on the use of indirect hormonal perturbations: A review of the literature. Int. J. Mol. Sci., 20(11): 2720. https://doi.org/10.3390/ijms20112720

Smith AK, Ropella GEP, McGill MR, Krishnan P, Dutta L, Kennedy RC, Jaeschke H, Hunt CA (2020). Contrasting model mechanisms of alanine aminotransferase release from damaged and necrotic hepatocytes as an example of general biomarker mechanisms. PLoS Comput. Biol., 16(6): e1007622. https://doi.org/10.1371/journal.pcbi.1007622

Venegas B, León Gordillo LY, Rosas G, Espinoza JA, Morán C, Domínguez R, Morales-Ledesma L (2019). In rats with estradiol valerate-induced polycystic ovary syndrome, the acute blockade of ovarian β-adrenoreceptors improve ovulation. Reprod. Biol. Endocrinol., 17: 95. https://doi.org/10.1186/s12958-019-0539-y

Xu X, Bai J, Liu K, Xiao L, Qin Y, Gao M, Liu Y (2023). Association of metabolic and endocrine disorders with bovine ovarian follicular cysts. Animals, 13(21): 3301. https://doi.org/10.3390/ani13213301

Yu Y, Tan P, Zhuang Z, Wang Z, Zhu L, Qiu R, Xu H (2021). DIA proteomics analysis through serum profiles reveals significant proteins as candidate biomarkers in women with PCOS. BMC Med. Genom., 14: 125. https://doi.org/10.1186/s12920-021-00962-7

Zhang Q, Lu XM, Zhang M, Yang CY, Lv SY, Li SF, Zhong CY, Geng SS (2021). Adverse effects of iron deficiency anemia on pregnancy outcome and offspring development and intervention of three iron supplements. Sci. Rep., 11(1): 1347. https://doi.org/10.1038/s41598-020-79971-y